



Effect of the oxygen deficiency on the physical properties of $\text{Ca}_2\text{MnO}_{4-\delta}$ compounds

N. Chihaoui^a, M. Bejar^a, E. Dharhi^{a,*}, M.A. Valente^b, M.P.F. Graça^b

^a Faculty of Sciences of Sfax, University of Sfax, Route Soukra Km 3.5, Sfax 3018, Tunisia

^b Physics Department-13N, University of Aveiro, 3810-193 Aveiro, Portugal

ARTICLE INFO

Article history:

Received 21 April 2011

Received in revised form 24 June 2011

Accepted 27 June 2011

Available online 2 July 2011

Keywords:

Oxygen-deficiency

EDAX spectra

Zero-field-cooled

Magnetization

Frustration

ABSTRACT

In this work, structural and magnetic studies have been investigated to explore the influence of the oxygen-deficiency (δ) on the physical properties of $\text{Ca}_2\text{MnO}_{4-\delta}$ ($\delta=0$ to 0.5) compounds. The samples cationic stoichiometry has been studied using energy dispersive X-ray analysis (EDAX). EDAX spectra, taken from the surface of the synthesized powders, have showed a nominal composition near the desired one. The structural study, by X-ray diffraction analysis, has confirmed the single-phase composition of all samples. The Rietveld refinement technique of the X-ray patterns, has revealed that samples crystallize in the tetragonal system with *I41/acd* space group for $\delta=0$ and in the orthorhombic one with *Bbcm* space group for $\delta>0$.

The applied magnetic field (μ_0H) and the temperature (T) dependences of the magnetization (M) have been studied using a vibrating sample magnetometer (VSM). From magnetization measurements versus temperature under the field-cooled (FC) and zero-field-cooled (ZFC) modes, we have deduced the presence of a spin-glass behavior characterized by a distinctive separation of the FC and ZFC curves. This behavior was found to become more important, as increasing the oxygen-deficiency δ , which leads to the appearance of magnetic frustration phenomenon.

© 2011 Elsevier B.V. All rights reserved.

1. Introduction

During the past decades, manganese-contained perovskite and Ruddlesden–Popper (RP) phases have been the subject of numerous studies because of their diverse behaviors including dielectric, magnetic and especially magnetoresistance, ionic conductivity, photocatalytic activity, luminescence and intercalations properties [1–6]. On the other hand, magnetic cooling by magnetocaloric (MC) effect has attracted much attention in the recent years [7–10] since it has a lot of advantages over gas refrigeration such as high efficiency, low noise, softer vibration and longer using time.

The RP phases, with the general formula $\text{A}_{n+1}\text{B}_n\text{O}_{3n+1}$ (A = lanthanide, alkaline earth, alkali metal; B = transition metal; $n = 1, 2, 3, \dots, \infty$) have structures consisting of alternate stacking of $n\text{ABO}_3$ perovskite block layers separated by an AO rock-salt-type layer [11,12]. The nature and the magnitude of these special properties can be modified by the choice of the cations A and B and of n , which depends on the synthesis conditions. Magnetism can be introduced by choosing a magnetic B ion [13,14]. Charge ordering

phenomena with strong consequences for the electronic conductivity result if the A-site is partially occupied by cations with two different charges and the B cation is multivalent [15–17], or if oxygen vacancies are formed in an oxygen-deficient environment [14]. One may even arrive at multifunctional materials in which the different functions are coupled if B is simultaneously magnetic and multivalent [18].

This work is focused on synthesis and characterization of $\text{Ca}_2\text{MnO}_{4-\delta}$ system. The parent compound, Ca_2MnO_4 , can be described as a succession of perovskite layers alternating with rock-salt (CaO) sheets along the crystallographic *c*-axis (Fig. 1). It was synthesized for the first time in polycrystalline form by Ruddlesden and Popper [11].

As known, the stoichiometric compound $\text{Ca}_2^{+2}\text{Mn}^{4+}\text{O}_4^{2-}$, containing only Mn^{4+} ions, is antiferromagnetic due to the super exchange coupling between Mn^{4+} ions. The classic method used to induce $\text{Mn}^{3+}/\text{Mn}^{4+}$ mixed valence involves substituting Ca^{2+} ion by a trivalent or tetravalent element [19–22]. However, it was found that this method induces a variation (increase or reduction) of the substituted sites radii, leading to an important modification of the structure and structural properties.

In order to avoid this problem, we propose a new method to introduce $\text{Mn}^{3+}/\text{Mn}^{4+}$ mixed valence by creation vacancies in

* Corresponding author. Tel.: +216 98373734; fax: +216 74676609.

E-mail address: essebti@yahoo.com (E. Dharhi).

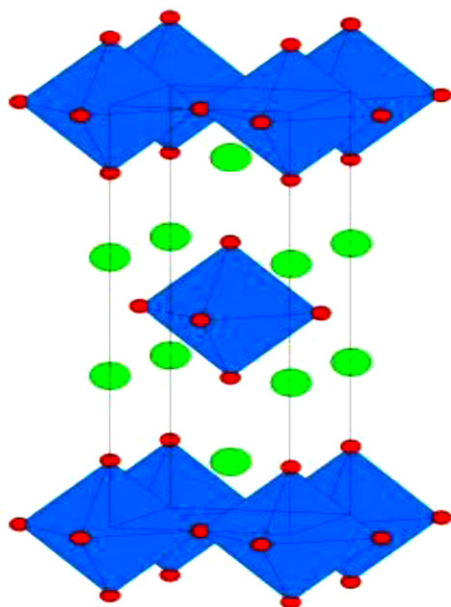


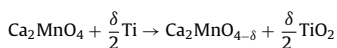
Fig. 1. Unit cell of Ca_2MnO_4 compound. Ca atoms are represented by green circles, while Mn atoms are at the center of the MnO_6 octahedra. (For interpretation of the references to color in this figure legend, the reader is referred to the web version of the article.)

the oxygen site. Thus, the radius of the A-site remains invariant, whereas that of the B-site changes.

2. Experimental

The $\text{Ca}_2\text{MnO}_{4-\delta}$ compounds ($\delta=0-0.5$) were synthesized in two steps:

- The Ca_2MnO_4 parent compound was prepared by the well known sol-gel technique. Stoichiometric amounts of $\text{Ca}(\text{NO}_3)_2$ (98%) and MnO_2 (99%) precursors were dissolved in a dilute HNO_3 solution with citric acid and ethylene glycol, used as chelating agents. The obtained mixture was then heated until a dark gel was formed. This gel was subsequently fired at 500°C and then at 700°C . The resultant powder was then subjected to three cycles of sintering for 48 h at 1000°C , 1100°C and 1200°C and a last cycle at 900°C for 10 days. Before every cycle, sample was carefully grinded and palletized with less than 2 tones/ cm^2 .
- In order to create vacancies in oxygen site, the Ca_2MnO_4 parent compound was placed in a quartz tube containing titanium in stoichiometric proportion according to the following reaction:



After that, the tube was pumped, sealed and annealed at 700°C for 15 days.

The cationic stoichiometry of the samples has been studied using energy dispersive X-ray analysis (EDAX).

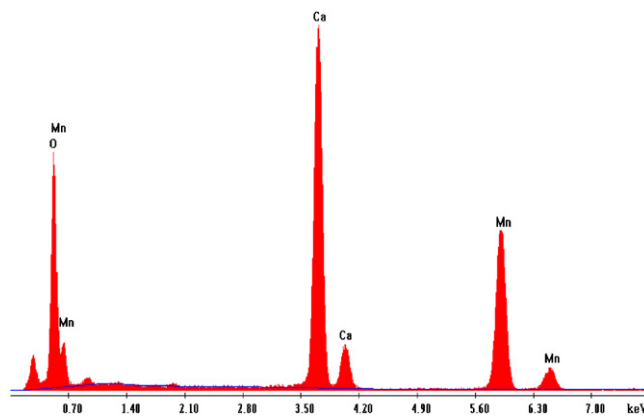


Fig. 2. Example of EDAX analysis spectral at room temperature for Ca_2MnO_4 ($\delta=0$) sample.

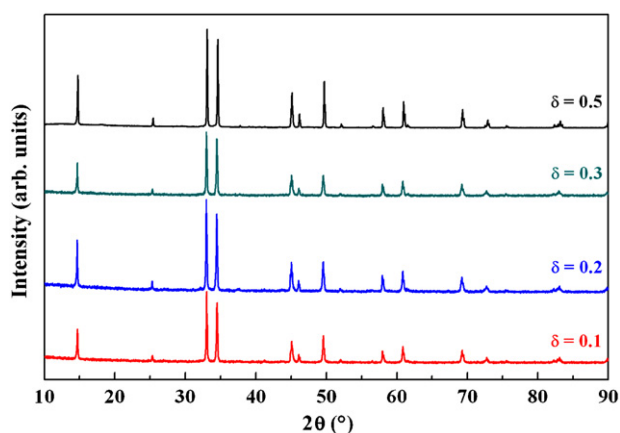


Fig. 3. X-ray diffraction (XRD) patterns at room temperature for $\text{Ca}_2\text{MnO}_{4-\delta}$ compounds ($\delta=0-0.5$).

The structure of the samples was characterized by X-ray diffraction at room temperature with $\text{Cu K}\alpha$ radiation ($\lambda = 1.5406 \text{ \AA}$) using a Siemens D5000 diffractometer. Data were collected over range of $10^\circ \leq 2\theta \leq 90^\circ$, with a step scanning of 0.01° and a counting time of 18 s per step. The data were analysed by the Rietveld method using the Fullprof program [23].

The temperature (T) dependence of the magnetization (M) was carried out with a VSM magnetometer in Physics Department-I3N, University of Aveiro. The magnetization data were collected after cooling the sample from 300 to 5 K in zero field cooling (ZFC) and in field cooling (FC) with a constant applied magnetic field of 0.1 T, respectively.

Table 1

Ca and Mn concentration values deduced from the EDAX analysis spectra realized at five different zones for $\text{Ca}_2\text{MnO}_{4-\delta}$ compounds ($\delta=0-0.5$).

| Zone | Element | Weight % | Atomic % | Ca concentration | Mn concentration |
|------|---------|----------|----------|------------------|------------------|
| 1 | CaK | 58.5 | 65.9 | 1.9718 | 1.0205 |
| | Mn | 41.5 | 34.1 | | |
| 2 | CaK | 60.5 | 67.8 | 2.0392 | 0.9713 |
| | Mn | 39.5 | 32.2 | | |
| 3 | CaK | 59.6 | 66.9 | 2.0089 | 0.9934 |
| | Mn | 40.4 | 33.1 | | |
| 4 | CaK | 58.3 | 65.7 | 1.9651 | 1.0254 |
| | Mn | 41.7 | 34.3 | | |
| 5 | CaK | 58.8 | 66.1 | 1.9819 | 1.0131 |
| | Mn | 41.2 | 33.9 | | |
| | | | | Mean value | Mean value |
| | | | | 1.9934 | 1.0047 |

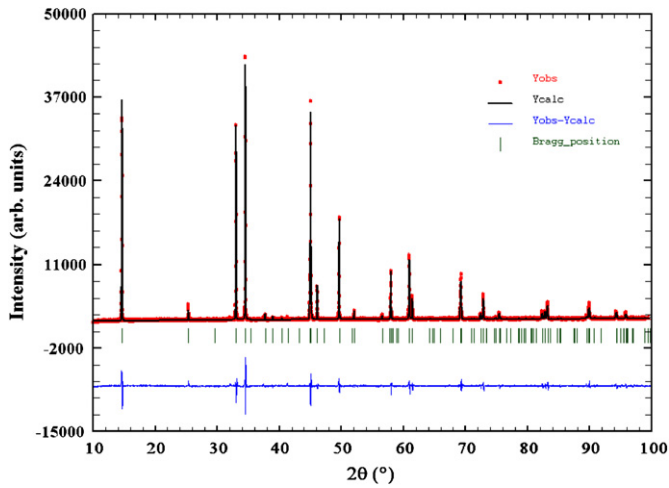


Fig. 4. Observed (solid circles) and calculated (solid line) XRD patterns of Ca_2MnO_4 ($\delta=0$) sample obtained at room temperature. The difference between these spectra is plotted at the bottom. Bragg reflections are indicated by ticks.

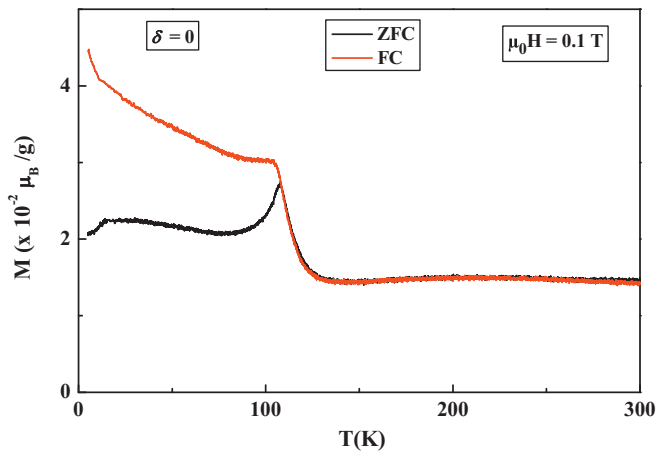


Fig. 5. Magnetization (M) as a function of temperature (T) for Ca_2MnO_4 ($\delta=0$) sample measured at applied magnetic field of 0.1 T under the field-cooled (FC) and zero-field-cooled (ZFC) modes.

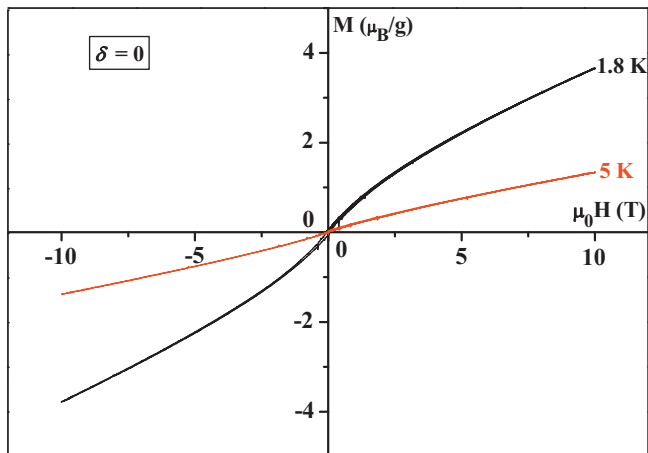


Fig. 6. Isothermal hysteresis loops at 1.8 and 5 K for Ca_2MnO_4 ($\delta=0$) sample.

3. Results and discussion

The composition of samples has been determined using energy dispersive X-ray analysis (EDAX). The EDAX spectra show the presence of Ca, Mn and O elements and did not contain any elemental impurities (Fig. 2). The analysis was performed on five different zones and has provided the results presented in Table 1.

The X-ray diffraction (XRD) analysis with Cu $K\alpha$ radiation at room temperature (Fig. 3) confirms single-phase composition of all samples. Using FULLPROF program [23], Rietveld refinement technique shows that the diffraction peaks corresponding to $\delta=0$ can be indexed in the tetragonal system with $I41/acd$ space group (Fig. 4). This result is in agreement with those found by Takahashi

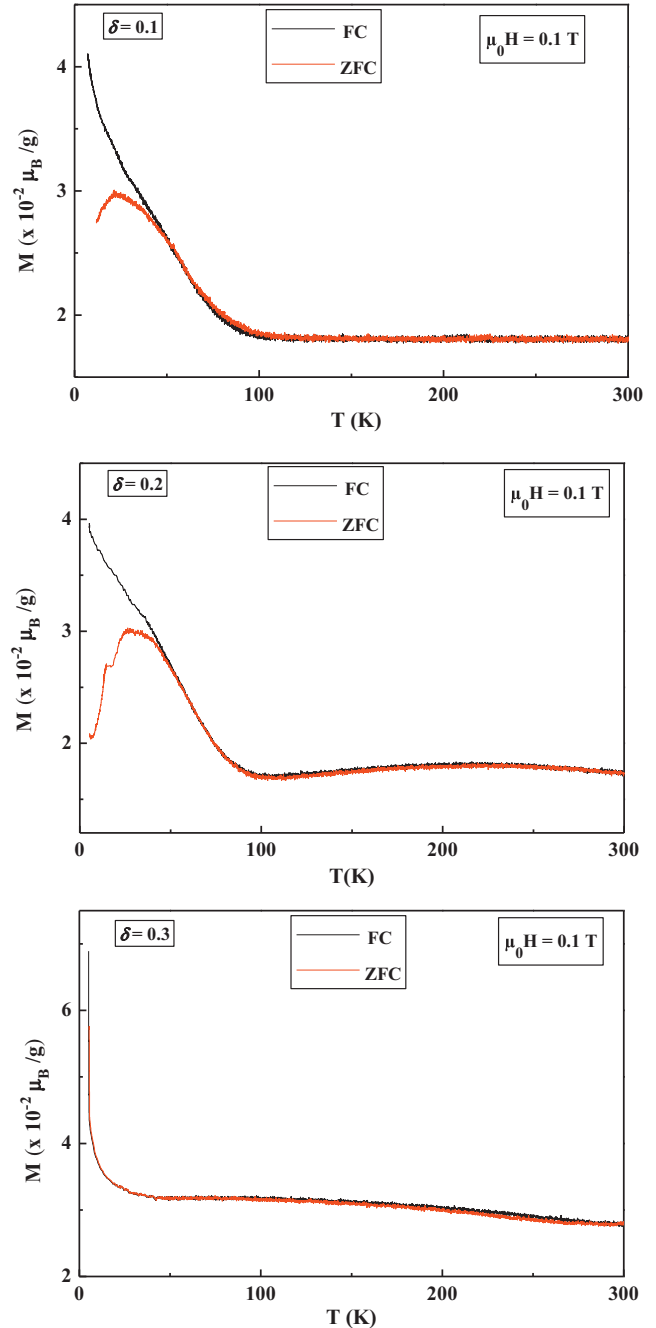


Fig. 7. Magnetization (M) as a function of temperature (T) for $\text{Ca}_2\text{MnO}_{4-\delta}$ ($\delta>0$) compounds measured at applied magnetic field of 0.1 T under the field-cooled (FC) and zero-field-cooled (ZFC) modes.

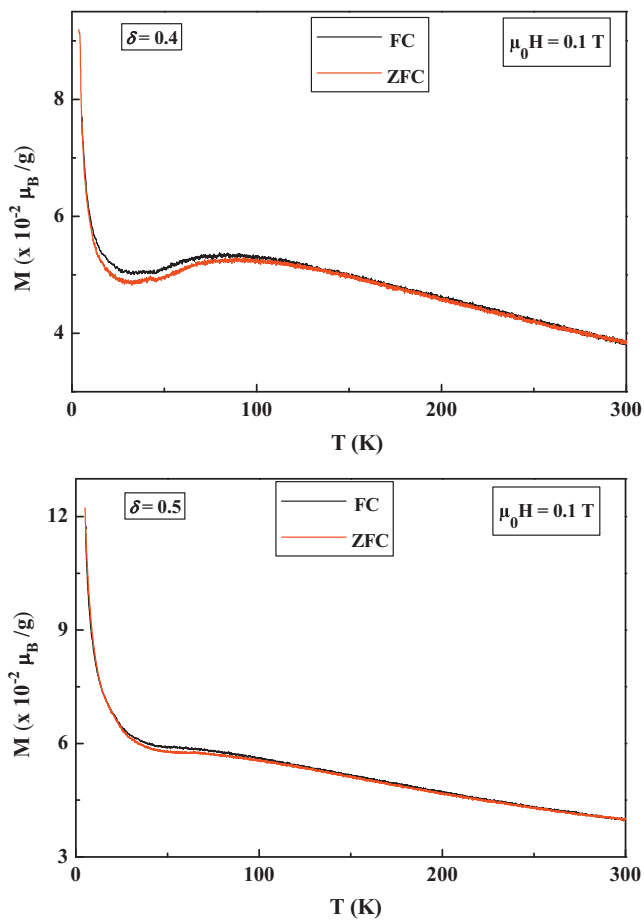


Fig. 7. (Continued.)

and Kamegashira [24] and Fawcett et al. [25]. The creation of oxygen defect generates several modifications and the diffraction peaks can be indexed in the orthorhombic system with *Bbcm* space group.

The dc magnetic measurements were carried out over a temperature (*T*) range of [5–300] K in an applied magnetic field (μ_0H) of 0.1 T both in zero-field-cooled (ZFC) and field-cooled (FC) modes. In ZFC mode, sample was cooled from room temperature to 5 K in zero magnetic field and at 5 K a magnetic field of 0.1 T was applied then measuring the magnetization (*M*) as the sample warmed up to 300 K. In the field cooled (FC) mode, sample was first cooled from 300 to 5 K under the magnetic field of 0.1 T and then *M* was measured in the warming process under the same field.

The dc magnetization data of Ca_2MnO_4 ($\delta=0$) sample as a function of temperature, collected at a magnetic applied field of 0.1 T, are shown in Fig. 5. As can be seen clearly, a cluster (spin) glass-like transition appears in the Ca_2MnO_4 sample, which is evidenced by a cusp in the ZFC curve at 113 K and a distinctive separation of the FC and ZFC curves. The dramatic difference between the ZFC and FC curves suggests that magnetic moments of Mn^{4+} ions order with a slight ferromagnetic component below Néel temperature. A similar *M(T)* plot was observed by Nagai et al. for the same compound [26].

Going deeper into the magnetic properties, the applied magnetic field (μ_0H) dependence of magnetization (*M*) at two different temperatures for $\delta=0$ sample is shown in Fig. 6. Our results reveal that *M*(μ_0H) curves do not show any saturation as μ_0H is as large as 10 T. The magnetization *M* versus μ_0H plot exhibits a small curvature at *T* = 1.8 K, which becomes less apparent at *T* = 5 K. This effect can be explained by the possibility of presence of an important antiferromagnetic interaction occurring at very low temperature (*T* < 1.8 K), which can persevere to the application of a magnetic field as large

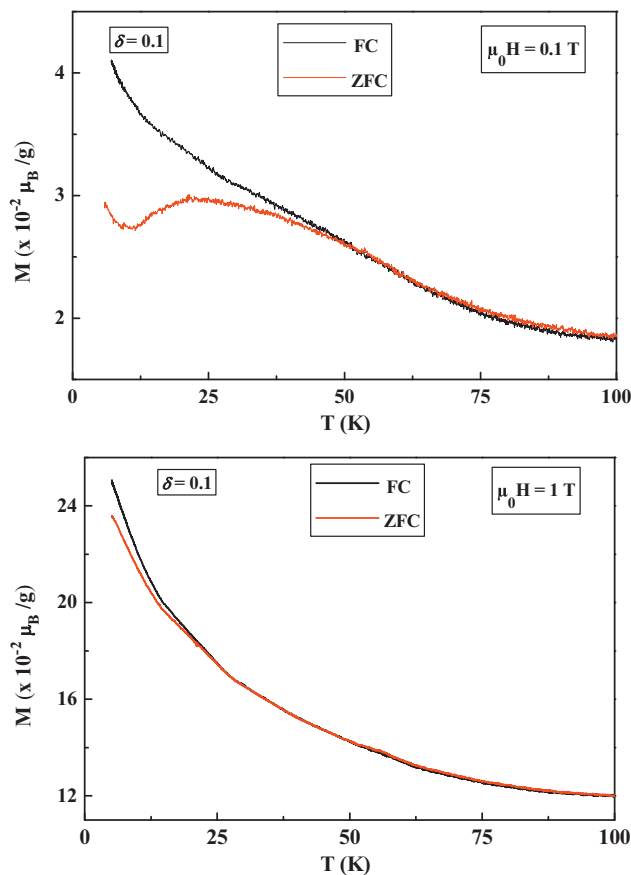


Fig. 8. Magnetization (*M*) as a function of temperature (*T*) for $\text{Ca}_2\text{MnO}_{3.9}$ ($\delta=0.1$) sample measured at two different applied magnetic fields under the field-cooled (FC) and zero-field-cooled (ZFC) modes.

as 10 T. As result, to observe magnetization saturation, we must make the measurement at temperature lower than 1.8 K.

The antiferromagnetic component is related to the presence of the spin-glass phenomenon, which is the result of random-looking mixture of positive and negative exchange interactions. This type of spin-glass interactions can occur in crystalline materials as well, where it can give rise to unusual magnetic behavior. Specifically, this type of interaction prevents the formation of a single-ordered magnetic ground state but rather tends to create a magnetic system with a large number of possible ground states. The spin-glass phenomenon is affected by the presence of the $\text{Mn}^{4+}/\text{Mn}^{3+}$ mixed valence.

Fig. 7 illustrates the variation of the magnetization (*M*) as a function of temperature (*T*) for $\text{Ca}_2\text{MnO}_{4-\delta}$ ($\delta>0$) compounds measured at applied magnetic field of 0.1 T under the field-cooled (FC) and zero-field-cooled (ZFC) modes. As shown, by increasing the rate of the oxygen-deficiency, the spin-glass behavior becomes more important and a phenomenon of magnetic frustration occurs. The blocking temperature (T_B) of this spin/cluster-glass behavior, revealed by the maximum of the ZFC curve, slightly changes from $T_B=113$ –25 K for $\delta=0$ and 0.2 samples, respectively. For more important values of the oxygen-deficiency, this transition will be observed at temperature lower than 5 K. For $\delta=0.1$ and 0.2 samples, the divergence between ZFC and FC curves starts around 50 K, which is above the blocking temperature (T_B). This is typical of spin glass, which have strong exchange interactions and/or short-ranged ordering occurring at higher temperatures, is in deep relation with the $\text{Mn}^{3+}/\text{Mn}^{4+}$ ratio, as mentioned previously. According to the electrical neutrality, the increase of the

oxygen deficiency content δ in $\text{Ca}_2^{2+}\text{Mn}_{1-2\delta}^{4+}\text{Mn}_{2\delta}^{3+}\text{O}_{4-\delta}^{2-}$ compounds leads to the increase of the Mn^{3+} ions number. Thus, as δ increases, there is augmentation of $\text{Mn}^{3+}/\text{Mn}^{4+}$ ratio leading to an enhancement of the spin-glass component and giving rise to a robust frustration magnetic phenomenon. This can give rise to the introduction of unusual magnetic behavior, which is generally accompanied by the absence of any magnetic transition as observed for samples with $\delta \geq 0.3$. It is noted that the ZFC and FC curves are not completely confused and they have a bifurcation for temperatures between 20 and 80 K for $\delta = 0.4$ and 25 and 75 K for $\delta = 0.50$ (Fig. 7). Thus, the frustration phenomenon, highlighted for $\delta \leq 0.2$, gives way to a thermomagnetic hysteresis phenomenon. Such irreversibility may be an indication of a viscosity increase of the spin correlations due to a freezing of the spin system.

We have studied the evolution of the spin-glass phenomenon as function of the applied magnetic field ($\mu_0 H$). Fig. 8 shows an example of the FC and ZFC magnetization curves for different applied magnetic fields for $\delta = 0.1$ sample. As can be seen, the increase of $\mu_0 H$ value leads to a decrease of the irreversibility temperature T_{irr} (temperature from which FC and ZFC curves coincide) from $T_{\text{irr}} = 50$ –21 K for $\mu_0 H = 0.1$ and 1 T, respectively. Also, we can note the decline of the blocking temperature to lower temperature.

4. Conclusions

The oxygen-deficiency effect on the structural and magnetic properties of $\text{Ca}_2\text{MnO}_{4-\delta}$ ($\delta = 0$ –0.5) compounds was investigated. These compounds have been characterized by energy dispersive X-ray analysis (EDAX), which has confirmed the stoichiometric of our samples. The structural study has exposed the presence of a monophasic *I41/acd* tetragonal structure for $\delta = 0$ sample. For $\delta > 0$ samples, the Rietveld refinements have showed that the structure remains monophasic and becomes orthorhombic with *Bbcm* space group. Magnetization measurements have revealed the presence of a spin-glass behavior illustrated by a distinctive separation of the field-cooled (FC) and zero-field-cooled (ZFC) curves. We have deduced that when increasing the oxygen-deficiency content δ , the spin-glass phenomenon becomes more important. As result, a robust frustration magnetic behavior takes place introducing a clear modification of the $M(T)$ curves.

Acknowledgements

This work, within the collaboration Tuniso–Portuguese framework, is supported by The Tunisian National Ministry of Higher Education, Scientific Research and Portuguese Agency for Science and Technology (FCT).

References

- [1] B. Raveau, A. Maignan, C. Martin, M. Hervieu, Chem. Mater. 10 (1998) 2641.
- [2] J. Sloan, P.D. Battle, M.A. Green, M.J. Rosseinsky, J.F. Vente, J. Solid State Chem. 138 (1998) 135.
- [3] Y. Tokura, Y. Tomioka, J. Magn. Mater. 200 (1999) 1.
- [4] F. Prado, A. Manthiram, J. Solid State Chem. 158 (2001) 307.
- [5] K. Boulahya, M. Parras, J.M. Gonzalez-Calbet, Chem. A Eur. J. 13 (2007) 910.
- [6] T. Hungria, I. MacLaren, H. Fuess, J. Galy, A. Castro, Mater. Lett. 62 (2008) 3095.
- [7] M. Bejar, R. Dhahri, F. El Halouani, E. Dhahri, J. Alloys Compd. 414 (1–2) (2006) 31.
- [8] M. Bejar, R. Dhahri, E. Dhahri, M. Balli, E.K. Hlil, J. Alloys Compd. 442 (1–2) (2007) 136.
- [9] N. Dhahri, A. Dhahri, K. Cherif, J. Dhahri, H. Belmabrouk, E. Dhahri, J. Alloys Compd. 507 (2010) 405.
- [10] M. Khliif, M. Bejar, O. El Sadek, E. Dhahri, M.A. Ahmed, E.K. Hlil, J. Alloys Compd. 509 (2011) 7410.
- [11] S.N. Ruddlesden, P. Popper, Acta Crystallogr. 10 (1957) 538.
- [12] S.N. Ruddlesden, P. Popper, Acta Crystallogr. 11 (1958) 54.
- [13] S.E. Dutton, M. Bahout, P.D. Battle, F. Tonus, V. Demange, J. Solid State Chem. 181 (2008) 2217.
- [14] L.J. Gillie, J. Hadermann, M. Hervieu, A. Maignan, C. Martin, Chem. Mater. 20 (2008) 6231.
- [15] Z. Jiao, X. Wan, H. Guo, J. Wang, B. Zhao, M. Wu, Ultramicroscopy 108 (2008) 1371.
- [16] L. Fawcett, E. Kim, M. Greenblatt, M. Croft, L. Bendersky, Phys. Rev. B 62 (2000) 6485.
- [17] W. Pickett, D. Singh, Phys. Rev. B 53 (1996) 1146.
- [18] J. Seidel, L. Martin, Q. He, Q. Zhan, Y. Chu, A. Rother, M. Hawkrigde, P. Maksymovych, P. Yu, M. Gajek, N. Balke, S. Kalinin, S. Gemming, F. Wang, G. Catalan, J. Scott, N. Spaldin, J. Orenstein, R. Ramesh, Nat. Mater. 8 (2009) 229.
- [19] N. Biskup, M. García-Hernández, I. Álvarez-Serrano, M.L. López, M.L. Veiga, J. Alloys Compd. 509 (2011) 4917.
- [20] M.T. Tlili, N. Chihaoui, M. Bejar, E. Dhahri, M.A. Valente, E.K. Hlil, J. Alloys Compd. 509 (2011) 6447.
- [21] A. Castro-Couceiro, M. Sanchez-Andujar, B. Rivas-Murias, J. Mira, J. Ivas, M.A. Sénaris-Rodríguez, Solid State Sci. 7 (2005) 905.
- [22] M.T. Tlili, M. Bejar, E. Dhahri, M.A. Valente, L.C. Costa, E.K. Hlil, Open Surf. Sci. J. 1 (2009) 54.
- [23] J. Rodriguez-Carvajal, Program FULLPROF.2K, Version 3.20, Institut Laue-Langevin, Grenoble, 2006.
- [24] J. Takahashi, N. Kamegashira, Mater. Res. Bull. 28 (1993) 565.
- [25] I.D. Fawcett, J.E. Sunstrom, M. Greenblatt, M. Craft, K.V. Ramanujachary, Chem. Mater. 10 (1998) 3643.
- [26] T. Nagai, A. Yamazaki, K. Kimoto, J. Alloys Compd. 453 (2008) 247.